INSIGHTS INTO BLOCKAGE, REVERBERATION AND DIRECTION FINDING USING ARRAY PROCESSING OF HYDROACOUSTIC SIGNALS IN THE INDIAN OCEAN

Jay J. Pulli, Zachary M. Upton, and Joydeep Bhattacharyya

BBN Technologies

ABSTRACT

BBN Technologies is currently tasked to improve the ability of the hydroacoustic community to model network performance using HydroCAM, the Hydroacoustic Coverage Assessment Model. Recent station installations in the Indian Ocean have yielded excellent data that allow us to evaluate and improve the models in HydroCAM. One of the resulting issues is that ray-based model predictions of hydroacoustic blockage do not always match what is seen in the data.

This year, BBN has focused on understanding blockage and developing a HydroCAM model that predicts blockage with greater accuracy. To achieve this goal, BBN is searching for very high-resolution bathymetry in areas near hydroacoustic stations, investigating model calculations of blockage to be integrated into HydroCAM, and leveraging its database of ground-truth events in the Indian Ocean to study blockage. We have obtained and integrated a 15-second bathymetry database near the site of the future station at Wake Island. We are still searching for high-resolution bathymetry databases near the active Indian Ocean stations at Diego Garcia and Cape Leeuwin.

To understand the effects of bathymetry on the received signals, we examined signals recorded by the International Monitoring System (IMS) arrays at Diego Garcia and Cape Leeuwin using array-processing techniques. Signals examined include seismic phases (*P* and *S* waves converted to acoustic energy below the arrays) and *T* waves from a number of earthquakes along the major tectonic features of the Indian Ocean. We used a modified version of the HydroTool component of MatSeis to compute both scrolling cross-correlations and frequency-wavenumber spectra for each event studied.

One of the events analyzed was the M_w 7.6 event on the Carlsberg Ridge on 15 July 2003. This event occurred on a nearly 200-km long fault break that was roughly perpendicular to the great circle path to Diego Garcia. Array analysis of the signals from this event indicate that the back-azimuth of the converted P and S waves point to the published epicenter, but the back-azimuth of the *T* wave points to the event centroid, 100 km from the epicenter, which is larger than the location error (as published by the Harvard Centroid Moment Tensor [CMT] project). This observation, confirmed by the analysis of a number of large events in our database, suggests that presumed back-azimuth biases of *T* waves might actually be attributed to the location differences between epicenter and centroid.

Array analysis of the *T* waves generated by the M_w 4.8 earthquake just west of the Chagos Archipelago on 25 July 2002 provides insight into the effect of back-scattering and reverberation on the back-azimuth calculations. This event produced *T* waves with a signal-to-noise ratio of 55 dB at the north array of Diego Garcia. However, only the first 10 percent of the *T* wave signal is coherent across the array. We attribute the incoherence of the remaining 90 percent of the *T* wave signal to backscatter from the Chagos Archipelago near the array. Ray-based blockage predictions for Diego Garcia indicate that the *T* waves from this event are blocked from reaching the south array. However, the *T* wave signal can be seen at amplitude that is 30 dB below that of the north array. Coherence and back-azimuth estimates for this smaller *T wave* signal are stable over a longer time-duration than for the larger signal at the north array. We attribute this stability to a lack of reverberation and back-scatter, since there are no significant bathymetric features behind the south array.

The array analysis of *T*-wave arrivals at Diego Garcia has yielded a better understanding of the capabilities and limitations of the array characteristics, *T*-wave generation, and the effects of blockage and reverberation on observed waveforms. Furthermore, the analysis of the 25 July 2002 event demonstrates the value of using signals that might appear to be blocked but that are, most probably, attenuated as the signals diffract around bathymetric features. In some cases, high amplitude arrivals do not demonstrate strong coherence across the array, but attenuated and diffracted signals may produce very coherent arrivals that can be used in back-azimuth calculations.

OBJECTIVES

The primary objective of this work is to support the Department of Energy (DOE) and the Air Force Technical Applications Center (AFTAC) in the use of the acoustic modeling program the Hydroacoustic Coverage Assessment Model (HydroCAM). Our previous work has shown that our predictions of hydroacoustic blockage using HydroCAM were inadequate to reflect the observations made at the hydrophone arrays in the Indian Ocean at Diego Garcia. Specifically, some paths that are predicted to be blocked are merely attenuated, with signals that are recorded and can be verified with travel-time calculations. In order to improve the model predictions, we have focused on two areas. First is the identification and integration into HydroCAM of high-resolution (<1-min grid) bathymetric data near the hydrophone stations. Second, we have been analyzing our Ground Truth Database of events in the Indian Ocean using array signal processing techniques in order to better understand the acoustic field around the receivers, especially the effects of refraction, diffraction, and reverberation.

Hydroacoustic blockage and diffraction of hydroacoustic energy around islands and seamounts is important to the evaluation of potential station locations and in the identification and classification of hydroacoustic arrivals. An improved modeling capability in HydroCAM will allow station planners and data analysts to better assess the detection and localization potential of the hydroacoustic network.

RESEARCH ACCOMPLISHED

High-Resolution Bathymetry

To better understand the effects of blockage, diffraction, and reverberation, BBN has been searching for high-resolution bathymetry data near the sites of International Monitoring System (IMS) hydroacoustic sensors. In prior modeling efforts (Pulli and Upton, 2001) the best resolution bathymetry available was the 2-min Sandwell and Smith bathymetry (Smith and Sandwell, 1997). This 2-min bathymetry represents a grid spacing of approximately 4 km. For smaller islands, atolls and seamounts, this resolution makes blockage prediction difficult. Also, even at the low frequency of 10 Hz, the wavelengths of acoustic energy are approximately 100 m, making a detailed study of blockage and diffraction difficult with these bathymetric data. While bathymetric data may never be collected near IMS hydroacoustic stations at a resolution less than 100 m, the research community will need greater resolution bathymetry in order to study its effects on hydroacoustic propagation in close proximity to the sensors.

The HydroCAM has been modified to use high-resolution bathymetric datasets near IMS stations in its hydroacoustic raypath calculations. The model uses these local datasets in conjunction with global, lower-resolution datasets to predict propagation and blockage on the ocean basin scale.

Bathymetric data at less than 1 arc-min resolution has been difficult to find, but we have had a few recent successes. During the site survey for the Wake Island IMS station, a 15sresolution grid was collected in a 3x3 degree area near the proposed station installation. These data have been integrated into HydroCAM. Figure 1 shows a cross section of the 15-second data compared to the same cross section using the Sandwell and Smith 2-min bathymetry.
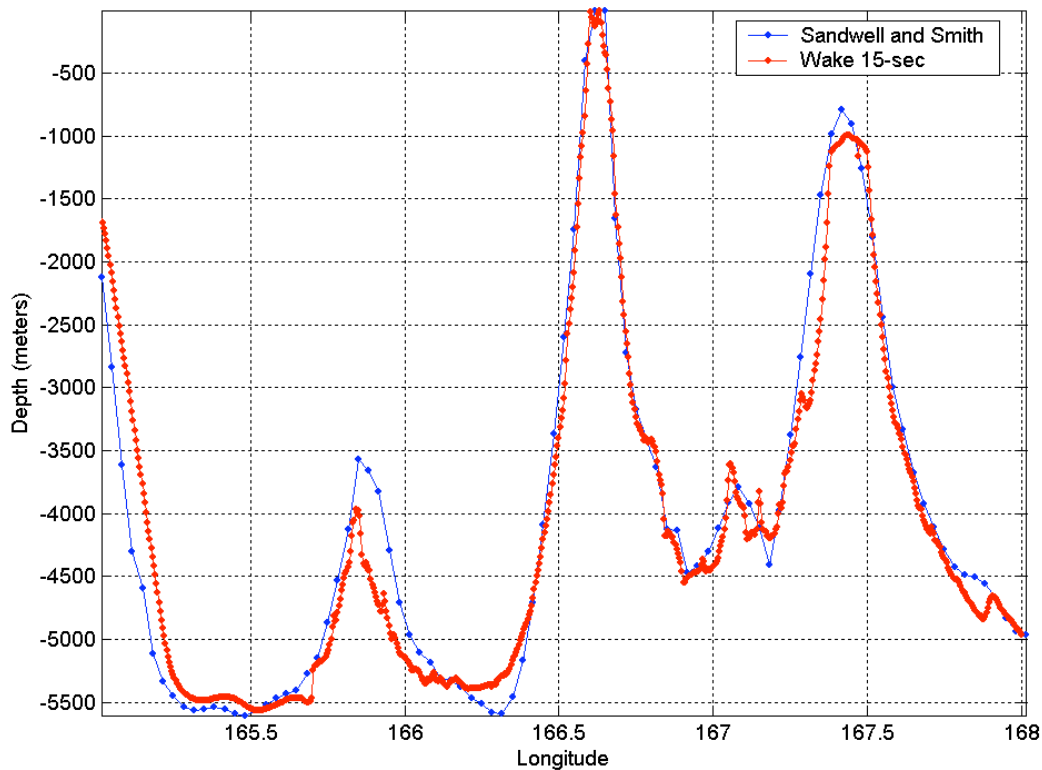
Figure 1. Bathymetric cross sections at 19.3° N Latitude. The red plot is at a 15-second resolution. The blue plot is at 2-min resolution

The IMS hydrophone station has not yet been installed at Wake Island. Therefore, we have delayed using these data in a detailed study of blockage. However, these data have been integrated into HydroCAM. As stated above, HydroCAM can now use the local high-resolution bathymetry in conjunction with global lower-resolution bathymetry in order to predict hydroacoustic raypaths.

We have also obtained a 36-second resolution bathymetric/topographic database of Australia and the surrounding waters, including the Cape Leeuwin (HA01) station location. These data are bounded by the coordinates: 8° S, 52° S, 102° E, 172° E and are a product of Geoscience Australia (Petkovic and Buchanan, 2002). The database represents over 900 surveys acquired since 1963 by Geoscience Australia, the Australian Hydrographic Service, oil exploration companies, and foreign institutions.

The Cape Leeuwin station has been receiving data since 2002. This bathymetric dataset could provide some valuable insight into local hydroacoustic propagation. Figure 2 shows the entire database. Figure 3 shows a subset of the data around the Cape Leeuwin station location. Figure 4 is a cross section comparison of the 9-second Geoscience Australia data and the 2-min Sandwell and Smith data. Of particular interest are the differences in the datasets. For example, note the areas in Figure 4 between -37.5 and –38° latitude or between –35 and –36° latitude.
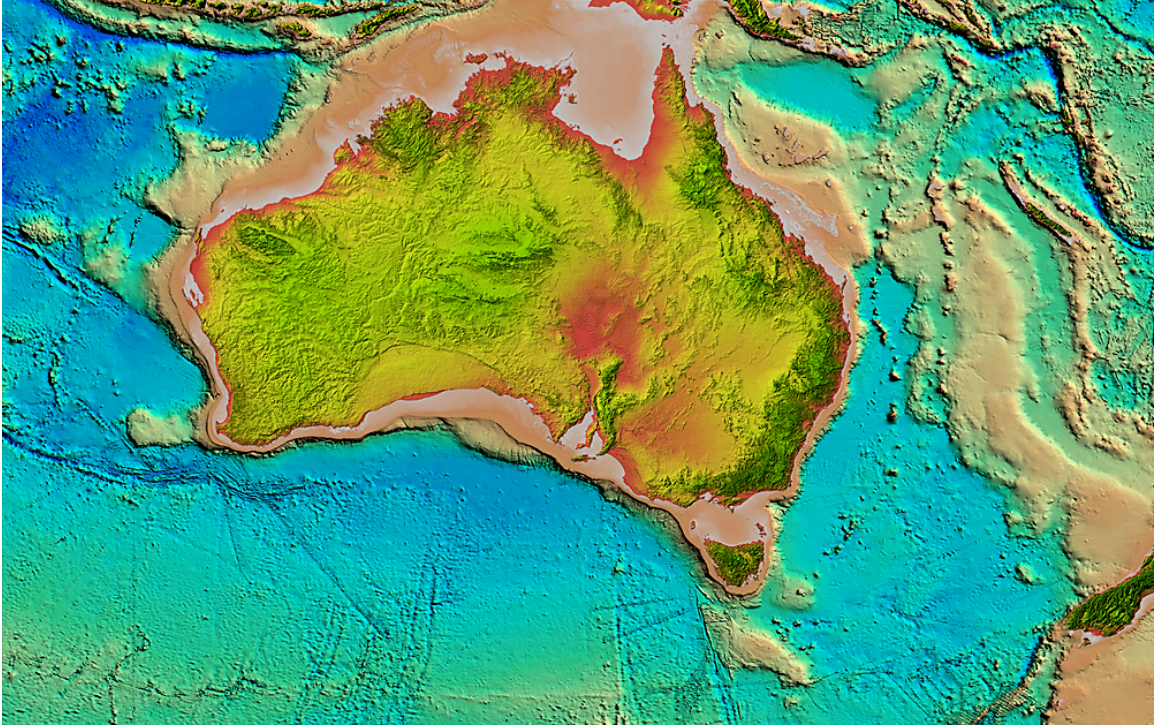
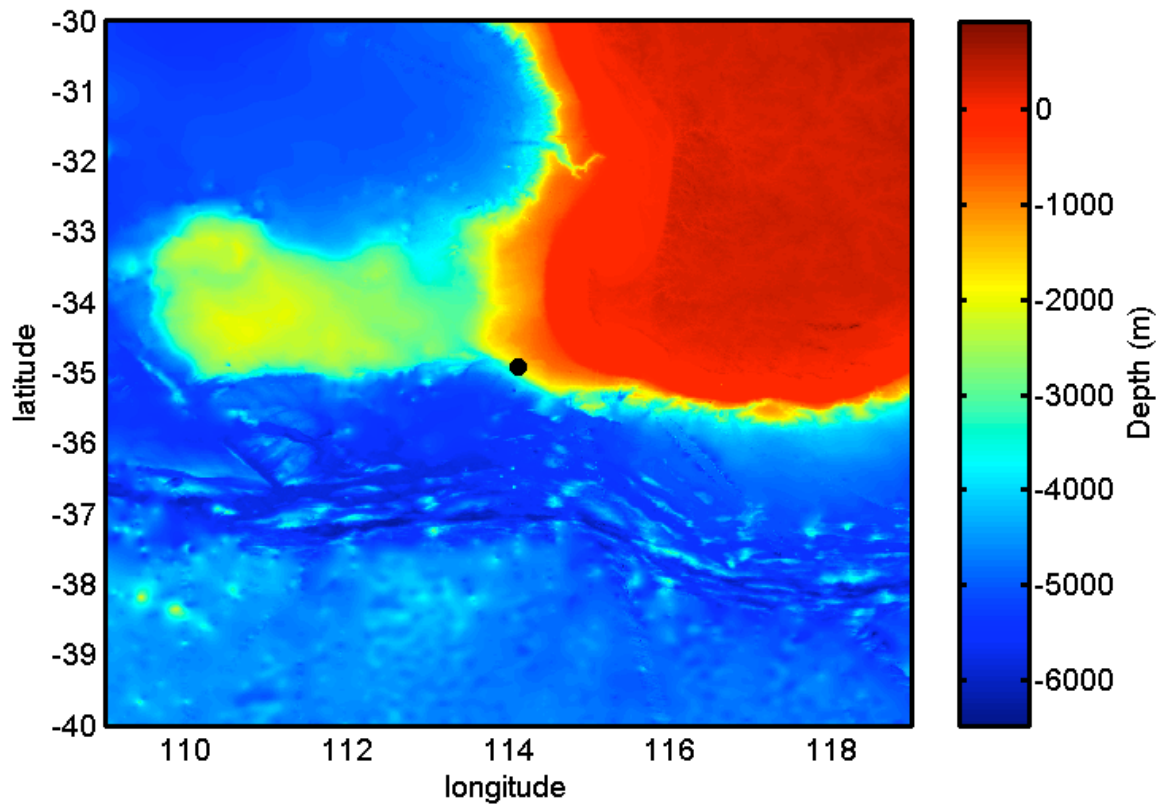**Figure 2. Geoscience Australia 36-second Bathymetry/Topography dataset**
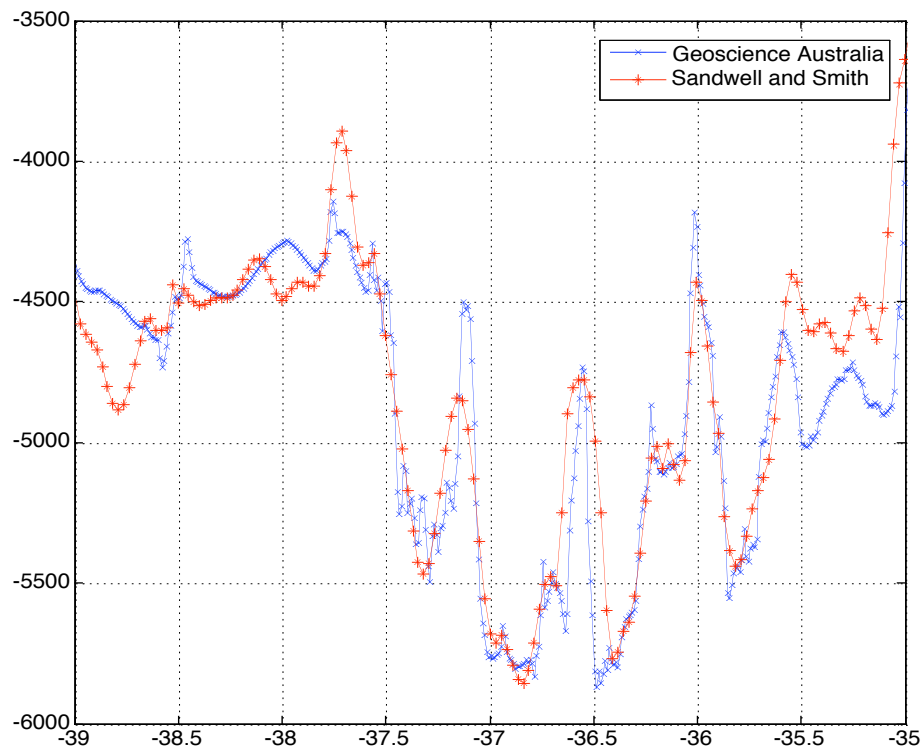

Figure 3. Geoscience Australia 36-second Bathymetry/Topography near Cape Leeuwin (HA01), which is represented by the black dot

Figure 4. Bathymetric cross-sections at 114° East Longitude. The blue plot is of the Geoscience Australia 36-second data; the red plot is of the 2-min Sandwell and Smith data.

The Geoscience Australia database is being integrated into HydroCAM as part of the HydroCAM 4.2 release. The HydroCAM 4.2 release will also include compatibility with Matlab version 7.0, a complete set of HTML-based tutorials, and many bug fixes and interface improvements.

Array Processing of Hydroacoustic Signals

Our ability to accurately predict hydroacoustic blockage will ultimately depend not only on the availability of high-resolution bathymetry near the source and receiver, but also on an understanding of actual propagation effects, including diffraction, refraction, and reverberation. This is best accomplished with an array of sensors, from which information about the propagating wavefield can be derived using array signal processing techniques. Although we are limited by the three-element configuration of the hydroacoustic arrays, we can derive information about signal coherence and propagation direction versus time in the *T* wave signal.

To accomplish this, we have used the hydroacoustic toolkit recently added to the program MatSeis (Merchant, et al., 2003). We processed the *T* wave signals, including the higher modes leading up to the Mode-1 peak of the *T*-wave and post Mode-1 *T*-wave coda, for approximately 25 Indian Ocean events recorded at Diego Garcia and Cape Leeuwin. The accompanying poster illustrates the analytical results for a number of these events, but here we will concentrate on the results of processing the *T*-wave data for two events located near the Diego Garcia arrays. These events occurred on 15 July 2003 on the Carlsberg Ridge, and on 25 July 2002 off the Carlsberg Ridge near the Chagos Archipelago. A map of these epicenters is shown in Figure 5.
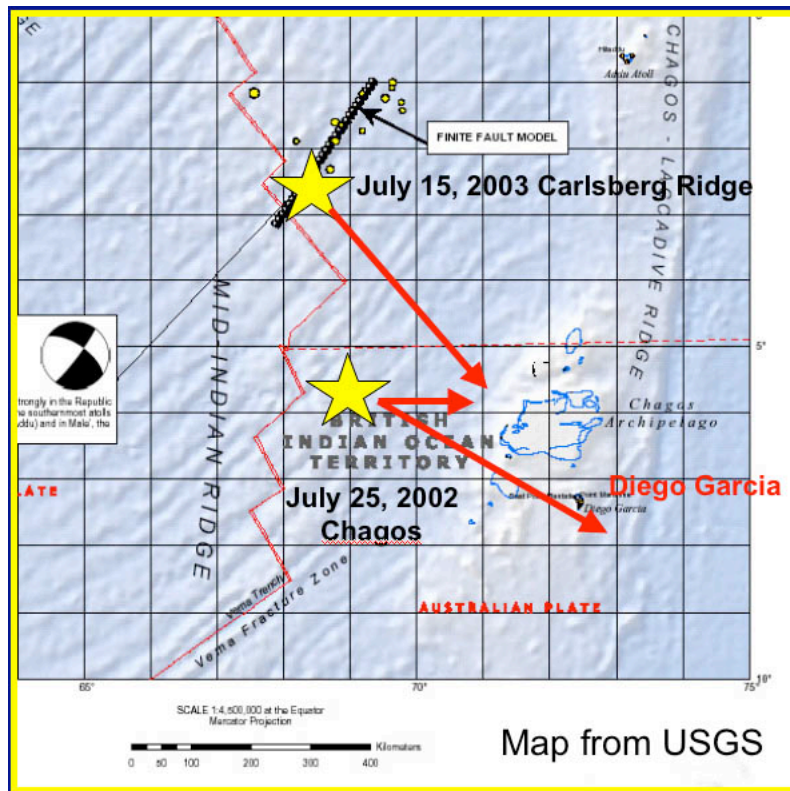
Figure 5. Epicentral map, adapted from a USGS map, illustrating the locations of the Carlsberg Ridge and Chagos Arch earthquakes, as well as the locations of the north and south hydroacoustic arrays at Diego Garcia.

For our analysis, we pre-filtered the data to a band of 3-50 Hz at each element. Scrolling cross-correlations were performed for 10-second windows with a 50% overlap. Figure 6 illustrates the result of this processing for the 15 July 2003 event on the Carlsberg Ridge, recorded on the north array at Diego Garcia. This event had a moment magnitude of 7.6, and the T wave signal had a peak signal-to-noise ratio at DGN of approximately 80 dB. Prior to the Mode-1 peak T-wave arrival at a travel time of 450s, the array processing indicates a stable back azimuth and apparent velocity estimate consistent with the actual back azimuth (330°) and acoustic velocity (1.5 km/sec). The only exceptions to this are the short windows around 325 and 375s, where the signal back azimuth is around zero degrees and the apparent velocity is unrealistically slow at 1 km/sec. After the Mode-1 arrival (> 450s), the signal-to-noise ratio is still high but signal coherence decreases, as indicated by the unstable back azimuth and apparent velocity. If we look at the map in Figure 5, we see that the Chagos Arch is approximately 100 km behind the DGN array, and back-scatter from this feature should begin to arrive at DGN at a two-way travel time of approximately 130s. This means that back scattered signals originating from near the start of our analysis window (320s) can interfere with the T wave signal after 450s.
°
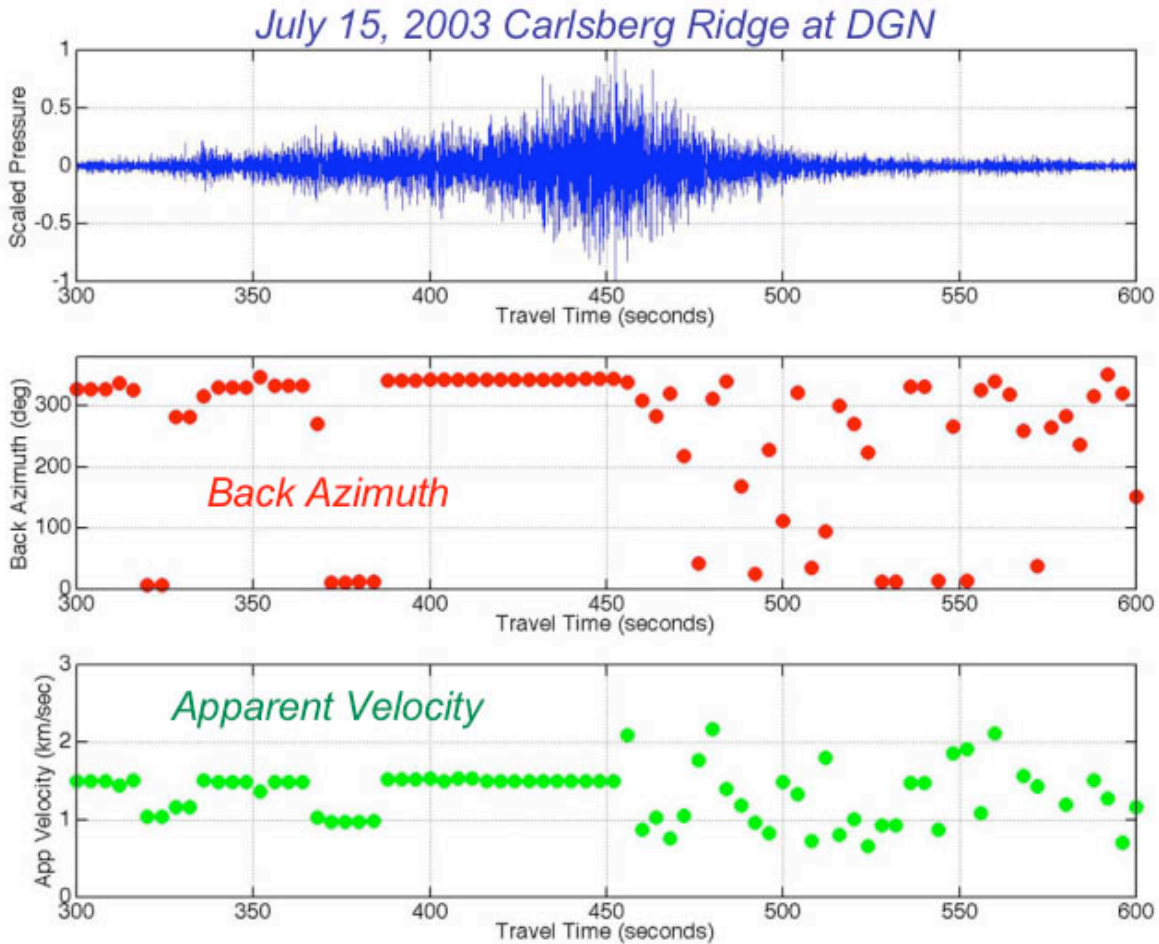
Figure 6. Array processing of the *T* wave signal for the 15 July 2003 earthquake on the Carlsberg Ridge recorded at Diego Garcia north. Three hundred seconds of data are included in the analysis. The Mode-1 peak arrives at the station at a travel time of 450s.

Our second example is that from the 25 July 2002 event off the Carlsberg Ridge near the Chagos Archipelago, shown in Figure 7. This was a smaller event, m_b=4.8, but closer to both Diego Garcia arrays. The *T* wave signal was well recorded at the north array, but is partially blocked on the south array. Array analysis of the data indicates that although the signal-to-noise ratio is high on the north array, the stability of the back azimuth is low, except for an approximately 25-second window just before the Mode-1 *T*-wave arrival at 225-seconds. Contrast this result with the observation at the south array, where the signal-to-noise ratio is much lower for the partially blocked signal. The back azimuth stability is significantly higher at the south station due to increased signal coherence. We hypothesize that this high coherence is due to the lack of back-scattered signals at the south array. Looking at the map in Figure 5, we see that there are no significant bathymetric features behind the south array to produce a back-scattered acoustic field. The back azimuth estimate is thus stable at 300° for nearly 140-seconds of recorded time, giving us robust signal detection.
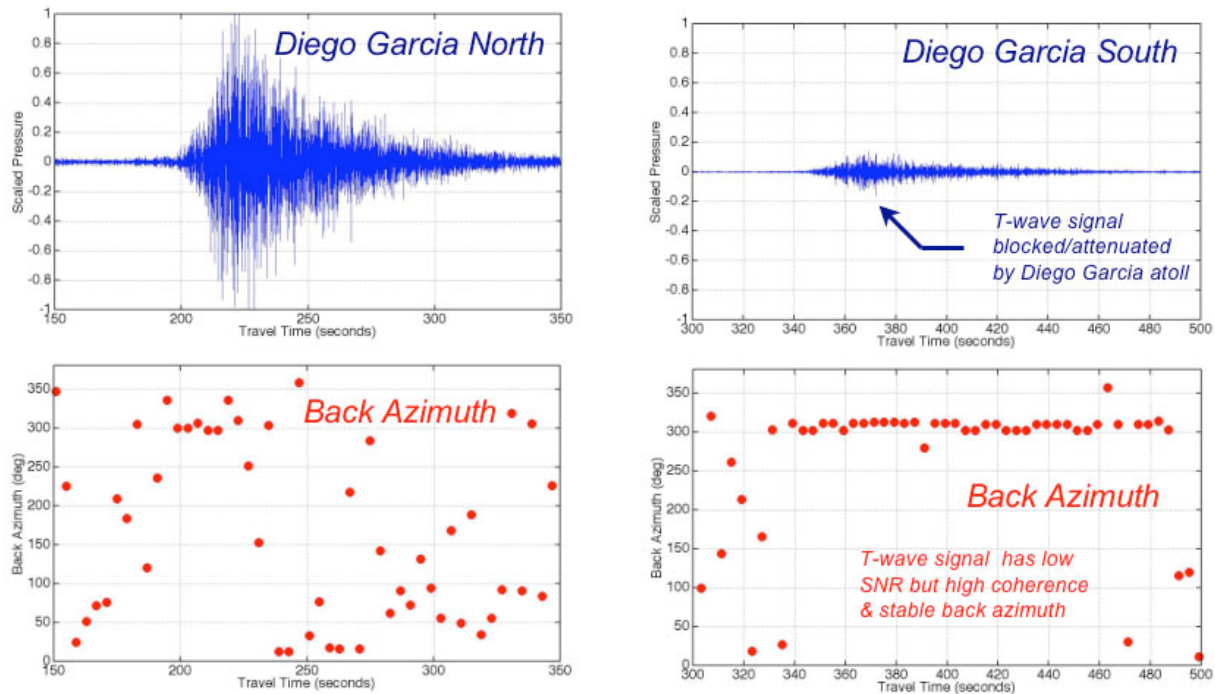
Figure 7. Array analysis at Diego Garcia north and south for the 25 July 2002 event off the Carlsberg Ridge. Although the signal level is high on the north array, the back azimuth estimate is unstable, due to the apparent interference effects of the back-scattered acoustic field from the Chagos Arch. The partially blocked signal on the south array is not affected by back-scatter interference, since there are no significant bathymetric features behind the array.

CONCLUSIONS AND RECOMMENDATIONS

We have identified and integrated two high-resolution bathymetric databases into HydroCAM. These data will allow researchers to better assess the effects of refraction, diffraction, and reverberation on the detection and localization capability of the hydroacoustic network. In addition, we have analyzed a number of hydroacoustic events from our Indian Ocean Ground Truth Database using array processing techniques. Our results illustrate the importance of backscatter and reverberation to the hydroacoustic field around the receivers, especially with respect to signal coherence and the determination of back azimuth.

Further study of these events will allow us to gain more insight into the nature of hydroacoustic blockage, diffraction and its prediction. A complete study, coupling the high-resolution bathymetry to the detailed data analysis is necessary to fully understand these effects on the acoustic field around the arrays.

REFERENCES

Petkovic, P. and C. Buchanan, (2002), *Australian bathymetry and topography grid*. Canberra: Geoscience Australia.

Pulli, J. J. and Z. M. Upton, (2001) "Hydroacoustic Blockage at Diego Garcia: Models and Observations," *Proceedings of the 23rd Seismic Research Review: Worldwide Monitoring of Nuclear Explosions*, pp. 45-54.

Smith, W. H. F. and D. T. Sandwell, (1997), Global Seafloor Topography from Satellite Altimetry and Ship Soundings, *Science*, 277, 1956-1962.

Merchant, B., E. Chael, C. Young (2003) "MatSeis and the GNEM R&E Regional Analysis Tools" in *Proceedings of the 25th Seismic Research Review – Nuclear Explosion Monitoring: Building the Knowledge Base,* Vol. II, pp. 721-728.